Finite-q antiferro-/ferri-magnetic toroidal order in a distorted kagome structure

Akimitsu Kirikoshi[1] and Satoru Hayami[2]

[1] *Research Institute for Interdisciplinary Science, Okayama University, Okayama 700-8530, Japan*

[2] *Graduate School of Science, Hokkaido University, Hokkaido 060-0810, Japan*

(Dated: April 18, 2025)

A highly geometrically frustrated lattice structure like a distorted kagome (or quasi-kagome) structure enriches physical phenomena through coupling with electronic structure, topology, and magnetism. Recently, it has been reported that an intermetallic HoAgGe exhibits two distinct magnetic structures with the finite magnetic vector $\boldsymbol{q} = (1/3, 1/3, 0)$: One is the partially ordered state in the intermediate-temperature region, and the other is the kagome spin ice state in the lowest-temperature region. We theoretically elucidate that the former is characterized by antiferro-magnetic toroidal ordering, while the latter is characterized by ferri-magnetic toroidal ordering based on the multipole representation theory, which provides an opposite interpretation to previous studies. We also show how antiferro-/ferri-magnetic toroidal orderings are microscopically formed by quantifying the magnetic toroidal moment activated in a multi-orbital system. As a result, we find that the degree of distortion for the kagome structure plays a significant role in determining the nature of antiferro-/ferri-magnetic toroidal orderings, which brings about the crossover between the antiferro-magnetic toroidal and the ferri-magnetic toroidal orders. We confirm such a tendency by evaluating the linear magnetoelectric effect. Our analysis can be applied irrespective of lattice structures and magnetic vectors without annoying the cluster origin.

A magnetic toroidal dipole (MTD), generated by a vortex structure of magnetic dipoles, is one of the fundamental quantities characterizing the antiferromagnetic structure. Since the MTD breaks both spatial inversion and time-reversal symmetries, the cross-correlated phenomenon known as the magnetoelectric (ME) effect has attracted considerable attention especially for antiferromagnetic insulators [1–3], e.g., Cr_2O_3 [4], $Ga_{2-x}Fe_xO_3$ [5, 6], $LiCoPO_4$ [7, 8], and $Ba_2CoGe_2O_7$ [9]. In recent years, the MTD order in metals has been studied intensively [10–12]. For example, the current-induced magnetization has been observed in UNi_4B [13] under the antiferromagnetic ordering with the MTD moment. Furthermore, transport phenomena characteristic of the MTD metals have been explored in both theory and experiment, such as nonreciprocal currents [14–16] and nonlinear Hall effects [17–20]. On the other hand, the antiferro(AF)-MTD order has attracted less attention since the cancellation of physical phenomena is anticipated. Indeed, no prototype materials have been reported so far.

Recently, the rare-earth compound HoAgGe has been proposed as a candidate for a new AF-magnetic toroidal metal, which exhibits a $\boldsymbol{q} = (1/3, 1/3, 0)$ magnetic structure in a $\sqrt{3} \times \sqrt{3}$ magnetic unit cell [21]. By decreasing the temperature from the paramagnetic state under the #189 $P\bar{6}2m$ ($D_{3\mathrm{h}}^3$) symmetry, this compound firstly shows the transition into the partially ordered state below 12 K, where 2/3 of Ho ions exhibit a vortex spin structure, and the remaining 1/3 of Ho ions are disordered, as shown in Fig. 1(a). When the temperature is further decreased to 7 K, all the Ho ions exhibit a complicated vortex spin structure, as shown in Fig. 1(b). Since this state consists of the triangles with the two-in/one-out or one-in/two-out configuration, it is referred to as the kagome spin ice state. Both magnetic phases are characterized by the same magnetic space group, $P\bar{6}'m2'$ [21]. Since the MTD belongs to the identity irre-

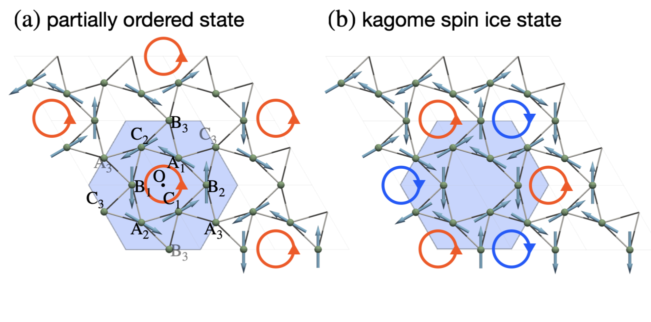

FIG. 1. Magnetic structures of (a) the partially ordered state and (b) the kagome spin ice state observed in HoAgGe [21]. The blue hexagon represents a magnetic ($\sqrt{3} \times \sqrt{3}$) unit cell with the origin O, and P_1-P_3 with $P = A, B, C$ are the labels of nine independent sites in the magnetic unit cell. The red counterclockwise (blue clockwise) arrows show a positive (negative) out-of-plane MTD moment defined by Eq. (1) at the center of each hexagon with six ordered magnetic moments.

ducible representation under $P\bar{6}'m2'$ [22], this compound can exhibit the MTD-related physical phenomena even for AF-magnetic/ferri-magnetic toroidal ordering, as detailed below.

The MTD moment has been defined in a conventional form as [21]

$$\boldsymbol{T}^{(\mathrm{c})} = \sum_i \boldsymbol{r}_i \times \boldsymbol{M}_i, \tag{1}$$

where $\boldsymbol{M}_i$ is the magnetic moment at the position $\boldsymbol{r}_i$ and the superscript (c) stands for the cluster quantity. When the cluster origin is set at the center of each hexagon, and the summation is taken for six sites on the hexagon like

[A$_1$-C$_2$-B$_1$-A$_2$-C$_1$-B$_2$ in Fig. 1(a)], one obtains the spatial distribution of the out-of-plane MTD moment as shown by clockwise or counterclockwise arrows in Figs. 1(a) and 1(b). This intuitive illustration of the MTD distribution indicates that the partially ordered state corresponds to the ferri-magnetic toroidal ordering, whereas the kagome spin ice state corresponds to the AF-magnetic toroidal ordering [21]. In contrast to such a simple picture, the evaluation of the MTD moment using Eq. (1) is ill-defined because the six sites consisting of the hexagon are not symmetry-related to each other owing to the lack of the sixfold rotational symmetry. Moreover, the cluster origin is arbitrarily taken within Eq. (1).

In this Letter, we investigate how to describe the MTD distribution under the finite-q magnetic structures without ambiguity based on the microscopic multipole representation theory [23, 24]. We show that the partially ordered and kagome spin ice states are expressed as the AF-magnetic and ferri-magnetic distributions of the MTD,which is opposed to the previous interpretation [21]. Then, we analyze a fundamental multi-orbital model to examine the spatial distribution of the MTD. We find that the degree of distortion for the kagome structure affects the behavior of the MTD; we show that the AF(ferri)-magnetic toroidal state in the perfect kagome structure turns into the ferri(AF)-magnetic toroidal state in the distorted kagome structure by changing the distortion parameter.

First, let us show how to describe AF- and ferri-magnetic toroidal ordering under the finite-q magnetic structure by adopting the symmetry-adapted multipole basis (SAMB) [24], which gives the symmetry-related correspondence between the multipole and electronic degrees of freedom under the $\boldsymbol{q} = \boldsymbol{0}$ structure independent of the choice of the cluster origin. Using the SAMB combined with the virtual cluster method, any three-sublattice magnetic structures can be expressed as a linear combination of six magnetic multipole bases M_i and three magnetic toroidal multipole bases T_i. Among them, the bases describing the in-plane spin modulations relevant to HoAgGe can be described by $\{|M_{01}\rangle, |T_{01}\rangle, |M_{03}\rangle, |M_{04}\rangle, |M_{05}\rangle, |M_{06}\rangle\}$, whereas the bases describing the out-of-plane spin modulations $\{|M_{02}\rangle, |T_{02}\rangle, |T_{03}\rangle\}$ are irrelevant in this study. We show the spin configurations corresponding to six bases in Fig. 2. The basis $|T_{01}\rangle$ corresponds to the MTD moment along the z direction, i.e., T_z, from the symmetry.

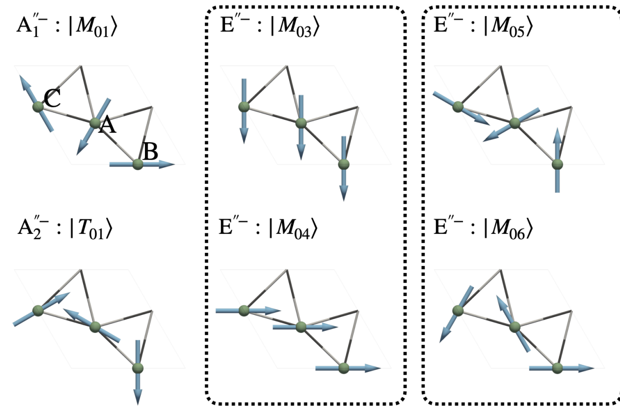

FIG. 2. SAMBs and their irreducible representations for the three-sublattice in-plane magnetic structure under the $D_{3\mathrm{h}}$ symmetry of the distorted kagome structure, where the superscript "$-$" represents odd parity for the time-reversal operation. The dashed lines enclose the bases for the two-dimensional irreducible representation E$''$.

The $\sqrt{3}\times\sqrt{3}$ magnetic structures in Fig. 1 can be constructed by taking the direct product of the spatial modulation with $\boldsymbol{q} = (1/3, 1/3, 0)$ and the three-sublattice SAMBs in Fig. 2 [25]. The basis corresponding to the partially ordered state in Fig. 1(a) is expressed by

$$|\mathrm{PO}\rangle = \frac{2}{3}\left(|T_{01}\rangle \sin\tilde{q}_- + |T'_{01}\rangle \sin\tilde{q}_+\right), \tag{2a}$$

whereas that for the kagome spin ice state is expressed as

$$|\mathrm{SI}\rangle = \frac{1}{3}|T_{01}\rangle - \frac{4}{3\sqrt{3}}(|T_{01}\rangle \cos\tilde{q}_- + |T'_{01}\rangle \cos\tilde{q}_+), \tag{2b}$$

with $|T'_{01}\rangle = \frac{1}{2}(|M_{03}\rangle - |M_{05}\rangle) + \frac{\sqrt{3}}{2}(|M_{04}\rangle - |M_{06}\rangle)$, and $\tilde{q}_\pm = \boldsymbol{q}\cdot\boldsymbol{r} \pm \pi/6$ for $\boldsymbol{q} = (1/3, 1/3, 0)$. It is noted that this finite-q expression is unique irrespective of the cluster origin. The correspondence between the other $\sqrt{3}\times\sqrt{3}$ magnetic structures and multipoles is shown in Supplemental Material (SM) [26].

The expression in Eq. (2a) indicates that the magnetic structure of the partially ordered state is characterized by the density wave of the MTD, meaning no $\boldsymbol{q} = \boldsymbol{0}$ component. In other words, the partially ordered state is regarded as the AF-magnetic toroidal state. On the other hand, the magnetic structure of the kagome spin ice state in Eq. (2b) includes the $\boldsymbol{q} = \boldsymbol{0}$ component as well as the finite-q one, which indicates the ferri-magnetic toroidal state. Thus, the symmetry-adapted argument suggests an interpretation that contrasts with the previous intuitive interpretation [21]. Indeed, recent experiments have shown that the nonlinear conductivity originating from the MTD becomes large in the kagome spin ice state with the ferri-magnetic toroidal structure, while that is negligibly small in the partially ordered state with the AF-magnetic toroidal structure [27].

Next, we quantify the MTD under the magnetic structures in Fig. 1. We here consider the multi-orbital model with different spatial parities to activate the MTD defined as the atomic-scale parity-mixing hybridization, e.g., s-p and p-d hybridizations. Specifically, we adopt the periodic Anderson model under the two-dimensional distorted kagome structure, which is given by

$$\mathcal{H} = \sum_{\boldsymbol{k}\eta\eta'\sigma} \varepsilon_{\boldsymbol{k}\eta\eta'} c^{\dagger}_{\boldsymbol{k}\eta\sigma} c_{\boldsymbol{k}\eta'\sigma} + \sum_{\boldsymbol{k}\eta\eta'\sigma\sigma'} (V^{\sigma\sigma'}_{\boldsymbol{k}\eta\eta'} c^{\dagger}_{\boldsymbol{k}\eta\sigma} p_{\boldsymbol{k}\eta'\sigma'} + \mathrm{H.c.}) + h \sum_{\boldsymbol{k}\eta\sigma\sigma'} T^{\sigma\sigma'}_{\eta} p^{\dagger}_{\boldsymbol{k}\eta\sigma} p_{\boldsymbol{k}\eta\sigma'}, \tag{3}$$

where $c^{\dagger}_{\boldsymbol{k}\eta\sigma}(c_{\boldsymbol{k}\eta\sigma})$ is the creation (annihilation) operator for the itinerant electron with momentum $\boldsymbol{k}$, sublattice $\eta \in \{\mathrm{A}_1, \mathrm{A}_2, \mathrm{A}_3, \mathrm{B}_1, \mathrm{B}_2, \mathrm{B}_3, \mathrm{C}_1, \mathrm{C}_2, \mathrm{C}_3\}$, and spin $\sigma = \pm 1$; $p^{\dagger}_{\boldsymbol{k}\eta\sigma}(p_{\boldsymbol{k}\eta\sigma})$ is that for the localized electron(σ represents the pseudospin). The sublattices $(\mathrm{A}_i, \mathrm{B}_i, \mathrm{C}_i)$ for $i = 1, 2, 3$ are connected by the three-fold rotation to each other, whereas $(\mathrm{P}_1, \mathrm{P}_2, \mathrm{P}_3)$ for $\mathrm{P} = \mathrm{A}, \mathrm{B}, \mathrm{C}$ are connected by the translation (See Fig. 1). The first term is the hopping term between the itinerant electrons

$$\varepsilon_{\boldsymbol{k}\eta\eta'} = t_s e^{i\boldsymbol{k}\cdot(\boldsymbol{r}_{\eta} - \boldsymbol{r}_{\eta'})}, \tag{4}$$

where t_s is the amplitude for the nearest-neighbor hopping and $\boldsymbol{r}_{\eta}$ is the position of the sublattice η in Fig. 1. The second term is the hopping between the itinerant electron at η with spin σ and the localized one at η' with pseudospin σ'. The coefficients is expressed as

$$V^{\sigma\sigma'}_{\boldsymbol{k}\eta\eta'} = t_{sp} e^{i\boldsymbol{k}\cdot(\boldsymbol{r}_{\eta} - \boldsymbol{r}_{\eta'})} w^{\sigma\sigma'}_{\eta\eta'}, \tag{5}$$

where t_{sp} is the amplitude for the nearest-neighbor hopping and $w^{\sigma\sigma'}_{\eta\eta'}$ is the overlap integral [26]. We suppose the orbital degrees for the itinerant and localized electrons are s and p orbitals, respectively, for simplicity, where we set the local crystalline electric field for the p (localized) orbital so that the magnetic easy axis is directed perpendicular to the mirror plane at each lattice site, as found in HoAgGe; see the detail in SM [26]. The third term represents the molecular field with the strength h to induce the partially ordered state or kagome spin ice state, which originates from the mean-field decoupling of the Coulomb interaction.

It is noteworthy that the degree of distortion from the perfect kagome structure affects the hopping between itinerant and localized electrons, reflecting the anisotropy of the localized orbital. To investigate the effect of the distortion on the MTD, we introduce the parameter δ as $\frac{1-\delta}{2}a(\frac{1}{2}, \frac{\sqrt{3}}{2})$ (a is the lattice constant of the unit cell in Fig. 1) for the A_1 site; the structure with $\delta = 0$ corresponds to the perfect kagome structure, and that with $\delta = 0.16$ corresponds to the distorted kagome structure in HoAgGe. We also show the coordinates for other sublattices in SM [26]. In the following calculation, we fix $t_s = -1, t_{sp} = 0.5$, $a = 1$, and the temperature $T = 10^{-3}$.

The atomic-scale operator of the z-component MTD per sublattice η is given by

$$T^{\eta}_{z} = \frac{1}{N_{\boldsymbol{k}}} \sum_{\boldsymbol{k}\sigma} (i c^{\dagger}_{\boldsymbol{k}\eta\sigma} p_{\boldsymbol{k}\eta\sigma} + \mathrm{H.c.}), \tag{6}$$

where $N_{\boldsymbol{k}}$ is the number of $\boldsymbol{k}$-mesh in the the Brillouin zone; we set $N_{\boldsymbol{k}} = 718^2$. Owing to the three-fold rotation around the z-axis for both the partially ordered and kagome spin ice states, the expectation value of T^{η}_{z}, $\langle T^{\eta}_{z} \rangle$, at $\eta = \mathrm{A}_i, \mathrm{B}_i, \mathrm{C}_i$ are equivalent.

Figures 3(a) and (b) show $\langle T^{\eta}_{z} \rangle$ for the partially ordered and kagome spin ice states, respectively, against the electron filling n and h. In the partially ordered state, the MTDs at the ordered sites (A_1 and A_2) are antiferroic, whereas that at the disordered sites (A_3) is relatively suppressed. This result means the antiferroic relation of the MTD satisfying $\langle T^{\mathrm{A}_1}_{z} \rangle = -\langle T^{\mathrm{A}_2}_{z} \rangle$ and $\langle T^{\mathrm{A}_3}_{z} \rangle \simeq 0$, as shown in Fig. 3(a). On the other hand, in the kagome spin ice state, the MTD at the A_1 and A_2 sites with the same magnetic moment shows a ferroic behavior over a wide parameter range, while the MTD at the A_3 site with the opposite magnetic moment tends to be developed in the opposite direction. This tendency of $\langle T^{\mathrm{A}_1}_{z} \rangle \simeq \langle T^{\mathrm{A}_2}_{z} \rangle \simeq -\langle T^{\mathrm{A}_3}_{z} \rangle$ holds for a wide parameter range, as shown in Fig. 3(b). These results are consistent with our symmetry-based interpretation of the AF-/ferri-magnetic toroidal ordering.

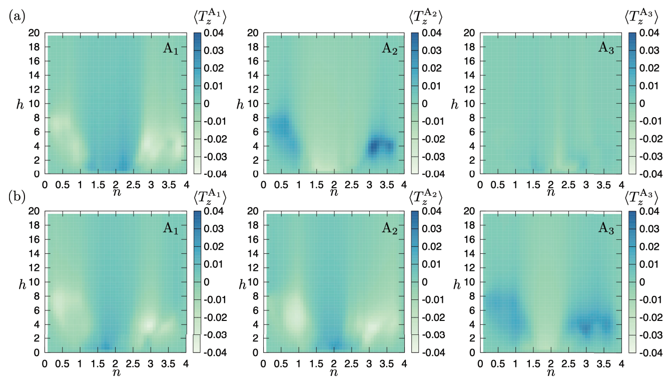

FIG. 3. The contour plot of the expectation values of the MTD T^{η}_{z} at each site in the filling n and molecular field h plane under (a) the partially ordered state and (b) the kagome spin ice state with $\delta = 0.16$.

Meanwhile, the relations of the $\langle T^{\mathrm{A}_1}_{z} \rangle = -\langle T^{\mathrm{A}_2}_{z} \rangle$ and $\langle T^{\mathrm{A}_3}_{z} \rangle = 0$ in the partially ordered state and $\langle T^{\mathrm{A}_1}_{z} \rangle = \langle T^{\mathrm{A}_2}_{z} \rangle = -\langle T^{\mathrm{A}_3}_{z} \rangle$ in the kagome spin ice state expected from the cluster multipole theory are violated in some parameter range. In order to understand the origin of such a deviation, we investigate the δ dependence of $\langle T^{\eta}_{z} \rangle$ in the left panel of Fig. 4. We find that the AF-magnetic toroidal and ferri-magnetic toroidal natures are transformed to each other by changing δ. For the perfect kagome structure with $\delta = 0$, we obtain the ferri(AF)-type distribution of the MTD, i.e., $\langle T^{\mathrm{A}_1}_{z} \rangle = \langle T^{\mathrm{A}_2}_{z} \rangle > 0$ and $\langle T^{\mathrm{A}_3}_{z} \rangle \neq 0$ ($\langle T^{\mathrm{A}_1}_{z} \rangle = -\langle T^{\mathrm{A}_2}_{z} \rangle$ and $\langle T^{\mathrm{A}_3}_{z} \rangle = 0$), rather than the AF(ferri)-type one in the partially ordered (kagome spin ice) state. This behavior for $\delta = 0$ is also understood from the SAMB under the perfect kagome lattice structure, as shown in SM [26].

When δ is nonzero, the MTD at each site changes so that its distribution in the partially ordered (kagome spin ice) state changes from the ferri(AF)-magnetic toroidal distribution to the AF(ferri)-magnetic toroidal one in a crossover way. By analytically analyzing the power dependence of δ in terms of $\langle T_z^\eta \rangle$ [28], we find that the even-order $O(\delta^{2n})$ contributes as $\langle T_z^{\mathrm{A}_1} \rangle = \langle T_z^{\mathrm{A}_2} \rangle \neq \langle T_z^{\mathrm{A}_3} \rangle$, whereas the odd-order $O(\delta^{2n+1})$ contributes as $\langle T_z^{\mathrm{A}_1} \rangle = -\langle T_z^{\mathrm{A}_2} \rangle$ and $\langle T_z^{\mathrm{A}_3} \rangle = 0$ in the partially ordered state. Similarly, we find that the even-order $O(\delta^{2n})$ contributes as $\langle T_z^{\mathrm{A}_1} \rangle = -\langle T_z^{\mathrm{A}_2} \rangle \neq 0$ and $\langle T_z^{\mathrm{A}_3} \rangle = 0$, whereas the odd-order $O(\delta^{2n+1})$ contributes as $\langle T_z^{\mathrm{A}_1} \rangle = \langle T_z^{\mathrm{A}_2} \rangle \neq 0$ and $\langle T_z^{\mathrm{A}_3} \rangle \neq 0$ in the kagome spin ice state. We show the schematic picture of the crossover between the ferri-magnetic toroidal and AF-magnetic toroidal order in the right panel of Fig. 4.

Finally, we relate the MTD distribution with the linear ME response. We evaluate the ME tensor defined by $M_\alpha = \chi_{\alpha\beta} E_\beta$ $(\alpha, \beta = x, y, z)$ from the Kubo formula. Since the magnetization can be decomposed into the sum of the contrbituions from each sublattice $M_\alpha = \sum_\eta M_\alpha^\eta$, the sublattice-dependent form is defined by

$$\chi_{\alpha\beta}^\eta = \frac{e\mu_{\mathrm{B}}\hbar}{iN_{\boldsymbol{k}}} \sum_{\boldsymbol{k}} \sum_{n\neq m} \frac{f_{n\boldsymbol{k}} - f_{m\boldsymbol{k}}}{(\varepsilon_{n\boldsymbol{k}} - \varepsilon_{m\boldsymbol{k}})^2} \mu_{\alpha\boldsymbol{k}}^{\eta,nm} v_{\beta\boldsymbol{k}}^{mn}, \qquad (7)$$

where $e > 0$ is the elementary charge, μ_{B} is the Bohr magneton, $\hbar$ is the Dirac constant, $\varepsilon_{n\boldsymbol{k}}$ is the band energy with the index n, $f_{n\boldsymbol{k}}$ is the Fermi–Dirac distribution function. $\mu_{\alpha\boldsymbol{k}}^{\eta,nm} = \langle n\boldsymbol{k}|\mu_\alpha^\eta|m\boldsymbol{k}\rangle$ with $\mu_\alpha^\eta = l_\alpha^\eta + 2s_\alpha^\eta$ is the band represenation of the magnetic moment operator at η and $v_{\beta\boldsymbol{k}}^{mn} = \hbar^{-1} \langle m\boldsymbol{k}|\partial_\beta h(\boldsymbol{k})|n\boldsymbol{k}\rangle$ is that of the velocity operator. We also define the total ME tensor as $\chi_{\alpha\beta}^{\mathrm{tot}} = \chi_{\alpha\beta}^{\mathrm{A}_1} + \chi_{\alpha\beta}^{\mathrm{A}_2} + \chi_{\alpha\beta}^{\mathrm{A}_3}$. Since nonzero T_z contributes to $\chi_{xy} = -\chi_{yx}$ [29, 30], we evaluate the antisymmetric component of χ_{xy}, that is, $\chi_{xy}^{(\mathrm{A})} = (\chi_{xy} - \chi_{yx})/2$ at each site. We set $e = \hbar = \mu_{\mathrm{B}} = 1$.

Figure 5 shows the δ dependence of $\chi^{(\mathrm{A})}$. For the kagome structure with $\delta = 0$, the total ME tensor is nonzero under the partially ordered state owing to the ferri-type MTD distribution. When the distorted kagome structure is considered, the site-resolved ME effect becomes large for the A_1 and A_2 sites, although they are canceled out with each other owing to the AF-type MTD distribution, as shown in Fig. 4(a). As a result, the total ME tensor is suppressed for all δ in the partially ordered state. On the other hand, the ME tensor is enhanced in the kagome spin ice state under the lattice distortion, as shown in Fig. 5(b), because the ferri-type MTD distribution with a net component is realized for $\delta \neq 0$. We also confirmed that the power of δ dependence of $\chi_{xy}^{(\mathrm{A})}$ is the same as that of the MTD moment for both magnetic orderings. In SM [26], we show the overall behavior of $\chi_{xy}^{(\mathrm{A})}$ for the filling and molecular field.

In summary, we theoretically investigated the foundations of the AF-magnetic and ferri-magnetic toroidal orderings under the finite-q magnetic structure. In the previous study [21], the spatial distribution of the local toroidal moment has been discussed based on Eq. (1), and they conclude that the partially ordered (kagome spin ice) state has a net (no) magnetic toroidal moment. However, applying the SAMBs to the two magnetic structures in HoAgGe, we found that the partially ordered state is characterized by the AF-magnetic toroidal distribution. In contrast, the kagome spin ice state is characterized by the ferri-magnetic toroidal distribution with the uniform component. By evaluating the spatial distribution of the atomic-scale MTD and linear ME tensor, we have shown that the lattice distortion parameter δ drives a crossover from the kagome structure-origin (even-power contribution of δ) to the distorted kagome structure-origin (odd-power contribution of δ). When the latter contribution is primary, the partially ordered state and the kagome spin ice state realized in HoAgGe are well characterized by the AF-magnetic toroidal and ferri-magnetic toroidal orderings, respectively. Our analysis will provide insight into the physical properties of the finite-q magnetic toroidal ordering in HoAgGe.

ACKNOWLEDGMENTS

The authors acknowledge T. Miyamoto, M. Shimozawa, S. Hosoi, and K. Izawa for fruitful discussions. This research was supported by JSPS KAKENHI Grants No. JP21H01037, No. JP22H00101, No. JP22H01183, No. JP23K03288, No. JP23H04869, No. JP23K20827, by JST CREST (JPMJCR23O4), and by JST FOREST (JPMJFR2366). Parts of the numerical calculations were performed in the supercomputing systems in ISSP, the University of Tokyo.

[1] C. Ederer and N. A. Spaldin, Phys. Rev. B **76**, 214404 (2007).
[2] N. A. Spaldin, M. Fiebig, and M. Mostovoy, J. Phys. Condens. Matter **20**, 434203 (2008).
[3] Y. V. Kopaev, Phys.-Uspekhi **52**, 1111 (2009).
[4] Y. F. Popov, A. M. Kadomtseva, D. V. Belov, G. P. Vorob'ev, and A. K. Zvezdin, J. Exp. Theor. Phys. Lett. **69**, 330 (1999).
[5] Y. F. Popov, A. M. Kadomtseva, G. P. Vorob'ev, V. A. Timofeeva, D. M. Ustinin, A. K. Zvezdin, and M. M. Tegeranchi, J. Exp. Theor. Phys. **87**, 146 (1998).
[6] T.-h. Arima, J.-H. Jung, M. Matsubara, M. Kubota, J.-P. He, Y. Kaneko, and Y. Tokura, J. Phys. Soc. Jpn. **74**, 1419 (2005).
[7] B. B. Van Aken, J.-P. Rivera, H. Schmid, and M. Fiebig, Nature **449**, 702 (2007).
[8] A. S. Zimmermann, D. Meier, and M. Fiebig, Nat. Commun. **5**, 4796 (2014).
[9] P. Toledano, D. D. Khalyavin, and L. C. Chapon, Phys. Rev. B **84**, 094421 (2011).

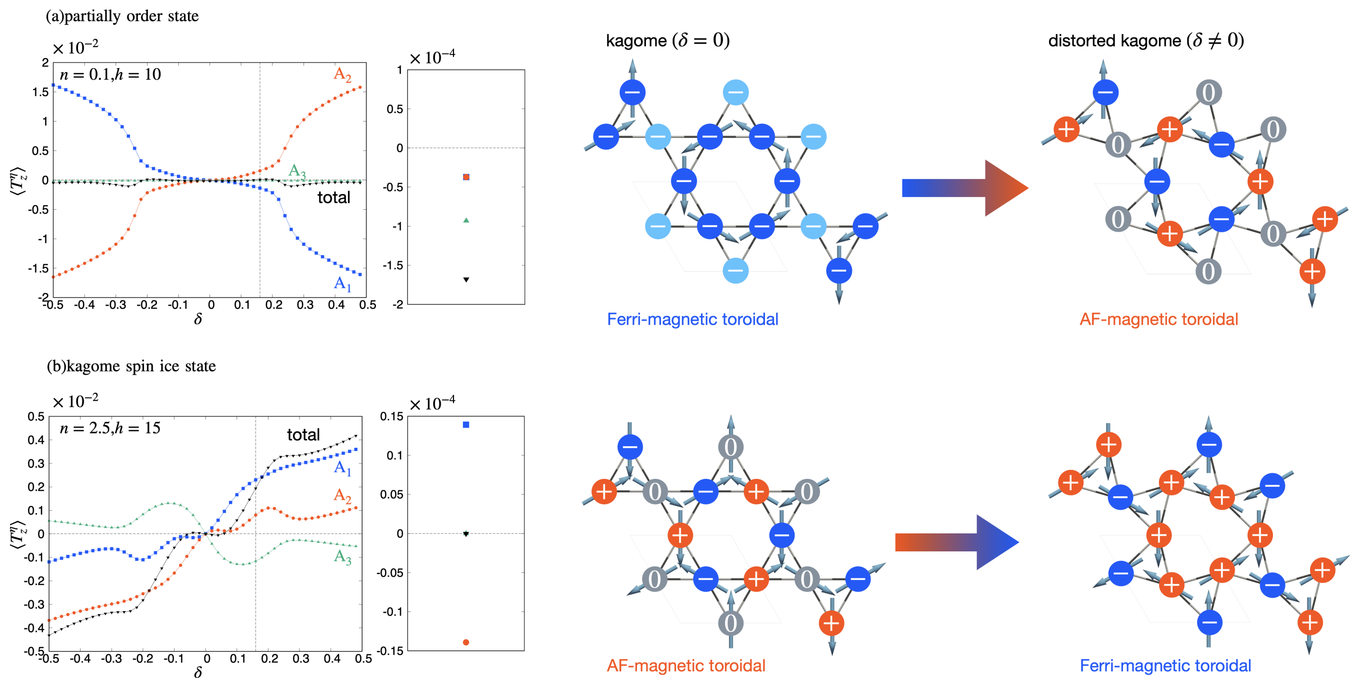

FIG. 4. Distortion parameter (δ) dependence of the MTD in Eq. (6) under (a) the partially ordered state and (b) the kagome spin ice state. The black points labeled as "total" are the rsults for $\langle T_1^{\mathrm{A}_1}\rangle + \langle T_1^{\mathrm{A}_2}\rangle + \langle T_1^{\mathrm{A}_3}\rangle$. The vertical dotted line at $\delta = 0.16$ indicates the case of HoAgGe. The second panels show the results at $\delta = 0$. The right panels show the schematic pictures of the change in the spatial distribution of the MTD, where the signs on each site represent the direction of the MTD.

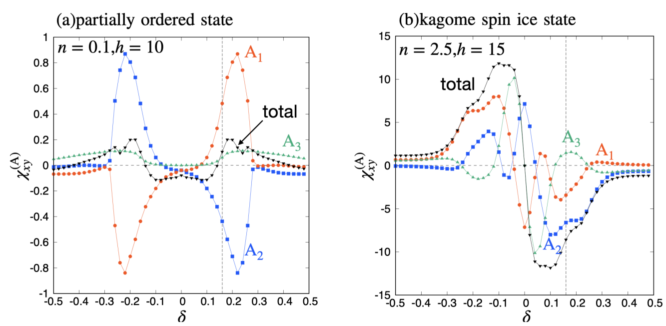

FIG. 5. Distortion parameter (δ) dependence of the ME tensor $\chi_{xy}^{(A)}$ per site and the sum of them, under (a) the partially ordered state and (b) the kagome spin ice state. The vertical dotted line at $\delta = 0.16$ indicates the case of HoAgGe. The parameters are the same as Fig. 4.

[10] Y. Yanase, J. Phys. Soc. Jpn. **83**, 014703 (2014).

[11] S. Hayami, H. Kusunose, and Y. Motome, Phys. Rev. B **90**, 024432 (2014).

[12] F. Thöle, A. Keliri, and N. A. Spaldin, J. Appl. Phys. **127**, 213905 (2020).

[13] H. Saito, K. Uenishi, N. Miura, C. Tabata, H. Hidaka, T. Yanagisawa, and H. Amitsuka, J. Phys. Soc. Jpn. **87**, 033702 (2018).

[14] H. Watanabe and Y. Yanase, Phys. Rev. Res. **2**, 043081 (2020).

[15] M. Yatsushiro, R. Oiwa, H. Kusunose, and S. Hayami, Phys. Rev. B **105**, 155157 (2022).

[16] Y. Suzuki, Phys. Rev. B **105**, 075201 (2022).

[17] C. Wang, Y. Gao, and D. Xiao, Phys. Rev. Lett. **127**, 277201 (2021).

[18] H. Liu, J. Zhao, Y.-X. Huang, W. Wu, X.-L. Sheng, C. Xiao, and S. A. Yang, Phys. Rev. Lett. **127**, 277202 (2021).

[19] A. Kirikoshi and S. Hayami, Phys. Rev. B **107**, 155109 (2023).

[20] K. Ota, M. Shimozawa, T. Muroya, T. Miyamoto, S. Hosoi, A. Nakamura, Y. Homma, F. Honda, D. Aoki, and K. Izawa, arXiv:2205.05555 (2024).

[21] K. Zhao, H. Deng, H. Chen, K. A. Ross, V. Petříček, G. Günther, M. Russina, V. Hutanu, and P. Gegenwart, Science **367**, 1218 (2020).

[22] M. Yatsushiro, H. Kusunose, and S. Hayami, Phys. Rev. B **104**, 054412 (2021).

[23] S. Hayami and H. Kusunose, J. Phys. Soc. Jpn. **93**, 072001 (2024).

[24] H. Kusunose, R. Oiwa, and S. Hayami, Phys. Rev. B **107**, 195118 (2023).

[25] Y. Yanagi, H. Kusunose, T. Nomoto, R. Arita, and M.-T. Suzuki, Phys. Rev. B **107**, 014407 (2023).

[26] See Supplemental Material, which includes Refs. [21, 22, 24, 25], for the symmetry-adapted multipole basis set, the local model Hamiltonian, the distortion parameter dependence of the sublattices, and the filling and molecular field dependence of the ME tensor.

[27] T. Miyamoto, S. Hosoi, M. Yatsushiro, K. Ota, K. Izawa, Y. Onuki, D. Aoki, S. Hayami, and M. Shimozawa (unpublished).

[28] R. Oiwa and H. Kusunose, J. Phys. Soc. Jpn. **91**, 014701 (2022).

[29] S. Hayami, M. Yatsushiro, Y. Yanagi, and H. Kusunose,

Phys. Rev. B **98**, 165110 (2018).

[30] H. Watanabe and Y. Yanase, Phys. Rev. B **98**, 245129 (2018).